

SCIENTIFIC REPORTS



OPEN

Adenovirus-mediated expression of orphan nuclear receptor NR4A2 targeting hepatic stellate cell attenuates liver fibrosis in rats

Received: 19 May 2016
Accepted: 24 August 2016
Published: 20 September 2016

Pengguo Chen^{1,2,3}, Jie Li¹, Yan Huo¹, Jin Lu¹, Lili Wan¹, Quanjun Yang¹, Jinlu Huang¹, Run Gan¹ & Cheng Guo^{1,2}

Liver fibrosis is a wound-healing response characterized with the accumulation of extracellular matrix (ECM). And hepatic stellate cells (HSCs) are the principal cell source of ECM. NR4A2 (Nurr1) is a member of orphan nuclear receptor NR4A family and acts as transcription factor. It participates in regulating cell differentiation, proliferation and apoptosis. We previously demonstrated that NR4A2 expression in fibrotic liver reduced significantly compared with normal liver and NR4A2 knockout in HSCs promoted ECM production. In the present study we explored the role of NR4A2 on liver fibrosis. Studies in cultured HSCs demonstrated that NR4A2 over-expression suppressed the activation of HSCs, such as ECM production and invasion ability. Moreover cell cycle was arrested, cell apoptosis was promoted and cell signaling pathway was influenced. Adenovirus-mediated delivery of NR4A2 in rats ameliorated significantly dimethylnitrosamine (DMN) induced liver fibrosis. The *In vivo* experiments produced results consistent with *in vitro* experiments. Taken together these results demonstrate NR4A2 enhancement attenuates liver fibrosis via suppressing the activation of HSCs and NR4A2 may be an ideal target for anti-fibrotic therapy.

Liver fibrosis is a wound-healing response characterized with the accumulation of extracellular matrix (ECM). An increase in the amount of the ECM is the typical feature of all forms of fibrosis. During liver fibrogenesis there is significant increase in the content of collagens, particularly of fibril-forming types I and III¹. The reiterated liver tissue damage due to infective (mostly hepatitis B and C viruses), toxic induced, metabolic and autoimmune can last for several decades and leads to cirrhosis, the end consequence of hepatic fibrosis, which has high mortality².

Epithelial mesenchymal transition (EMT) has been closely related to liver fibrogenesis through which epithelial cells contribute to the replacement of dead or damaged hepatic cells^{3–5}. The ECM is mostly produced by myofibroblasts. HSCs (hepatic stellate cells) are the key myofibroblast population in hepatic fibrosis. It was reported that 94% to 96% of myofibroblasts were derived from HSCs in liver fibrotic models and the contribution of HSCs to the hepatic myofibroblast pool in liver fibrosis ranged from 82% to 89%⁶.

HSCs reside in the space of Disse which constitute 5–15% of all hepatic cells and represent a vital fibrogenic cell population in liver. HSCs store retinyl esters in intracytoplasmic lipid droplets and exhibit features of vascular pericytes regulating sinusoidal blood flow and produce significantly more ECM than parenchymal cells^{7–9}.

Both in animal models and human beings, it has been proved that liver fibrosis is reversible with treatment not limited to cessation of the causative agent^{10–13}. Targeting both specific functions of myofibroblast (collagen production) and myofibroblast themselves might prove therapeutically effective. HSCs are not only a key fibrogenic cell population in the liver but also amenable to cell-specific delivery approaches which makes them an attractive candidates for direct anti-fibrotic therapy¹⁴.

NR4A2 (also called Nurr1) is a member of orphan nuclear receptor NR4A family and acts as transcription factor. The NR4A subfamily members are widely distributed in cells regulating differentiation, proliferation and apoptosis and involved in multiple diseases, for example vascular sclerosis, cancer and metabolic syndrome. Our

¹Department of Pharmacy, Shanghai Jiao Tong University Affiliated Sixth People's Hospital, 600 Yishan Road, Shanghai, China. ²Shanghai Jiao Tong University School of Medicine, Shanghai, China. ³Department of Gastroenterology, Jiangxi Provincial People's Hospital, 92 Aiguo Road, Nanchang, Jiangxi, China. Correspondence and requests for materials should be addressed to C.G. (email: guopharm@126.com)

previous study demonstrated NR4A2 knockdown could promote HSCs proliferation¹⁵. In this study we explored the effect of AdNR4A2, adenovirus carrying NR4A2 gene, on activated HSCs or liver fibrosis and clarified its mechanism. Our data showed that NR4A2 gene over-expression by adenovirus-mediated significantly suppressed the activated HSCs and attenuated dimethylnitrosamine (DMN) reduced hepatic fibrosis. These results suggest that NR4A2 could be a promising target gene for anti-fibrotic therapy and exploiting agents that increases NR4A2 expression would be very meaningful.

Results

AdNR4A2 decreases the expression of ECM gene in HSCs. In liver fibrosis, activated HSCs produced most ECM and the level of α smooth muscle actin (α -SMA), a typical marker for liver fibrosis elevates significantly.

To investigate the effect of NR4A2 on ECM production AdNR4A2 and its negative control AdNC were generated. We verified the MOI (Multiplicity of Infection) of AdNR4A2 and AdNC in HSCs and the preferred MOI was 40. RT-PCR analysis showed the NR4A2 mRNA expression in HSCs infected with AdNR4A2 was 100 times higher than in cells infected with AdNC (Fig. 1a). Meantime the α -SMA level decreased significantly by 70% (Fig. 1b). The results demonstrated that ECM production was restrained after NR4A2 enhancement in HSC-T6 cells.

Furthermore we investigated the influence of AdNR4A2 on primary hepatic stellate cells. Primary hepatic stellate cells could activate spontaneously after isolation that resembles the activation process *in vivo*¹⁶. We isolated primary hepatic stellate cells from SD-rats and on the third day AdNR4A2 or AdNC infected the primary hepatic stellate cells respectively. RT-PCR results showed that NR4A2 mRNA level increased by 300-fold and α -SMA level reduced by 50% in AdNR4A2 treated cells than in AdNC treated cells (Fig. 1c,d). These data implied that NR4A2 may inhibit ECM production *in vivo*.

TGF- β plays a central role in activating HSCs and induces the transcription of type I and III collagen which are important components of ECM¹⁷. RT-PCR analysis showed the TGF- β mRNA expression reduced by more than 60% in AdNR4A2 treated cells than in AdNC treated cells (Fig. 1e). Meanwhile the Col I and Col III level decreased by 40% and 20% respectively after NR4A2 enhancement in HSCs (Fig. 1f,g).

AdNR4A2 arrests cell cycle and promotes HSCs apoptosis. During fibrosis reversion stage activated HSCs revert to quiet state or even apoptosis. To explore whether AdNR4A2 promote cell apoptosis or prohibit cell proliferation, AdNR4A2 or AdNC infected HSCs respectively for 48 hour. FACS analysis of propidium iodide-stained cells revealed that AdNR4A2 treatment caused significant cellular accumulation in G1 phase and reduced percentage in S phase compared with AdNC treatment (Fig. 2a,b and Supplementary Fig. S1a,b,c).

Meanwhile we investigated the influence of AdNR4A2 on cell apoptosis. FACS for cell apoptosis assay showed that cell apoptosis rate increased significantly from about 2–3% to 22% in AdNR4A2 infected cells than in AdNC infected cells (Fig. 2c,d and Supplementary Fig. S1d,e,f). Above results confirmed that AdNR4A2 promoted markedly cell apoptosis apart from arresting cell cycle in HSCs.

AdNR4A2 inhibits cell migration. In liver fibrogenesis HSCs also contribute to angiogenesis regeneration. Activated HSCs migrate along with endothelial cells to establish vascular connections which lead to creating new sinusoidal branches¹⁸.

In order to assess whether AdNR4A2 inhibit HSCs from migrating transwell migration assays were employed. Transwell results showed that cell migration ability was weakened significantly after AdNR4A2 treatment (Fig. 3a,b). It implied that AdNR4A2 could suppress the migration of activated HSCs.

AdNR4A2 increases the phosphorylation of ERK1/2 and P38 in HSCs. During the activation of HSCs multiple signaling pathways play important role. And among them MAPK pathway is vital for the activation of HSCs¹⁹. MAPK family includes extracellular signal-regulated kinase (ERK), c-Jun N-terminal kinase (JNK) and P38.

We explored the effect of AdNR4A2 on phosphorylation of MAPK. AdNR4A2 or AdNC infected HSC-T6 cells respectively for 72 hour. The Western blot results showed increased phosphorylation of ERK and P38 after AdNR4A2 treatment (Fig. 4a,b). The data suggested that AdNR4A2 may activate MAPK signaling pathway in HSCs to suppress the activated HSCs.

AdNR4A2 increases the export of nucleus of NR4A2. Orphan nuclear receptor NR4A2 mostly locates in nucleus. The translocation from nucleus to cytoplasm, such as mitochondria, triggers release of cytochrome C which results in the cell apoptosis²⁰. To verify the correlation between AdNR4A2 promoted cell apoptosis and the nucleus export of NR4A2 in HSCs cell immunofluorescence assay was performed.

Our results indicated the rate of NR4A2 nuclear translocation in AdNR4A2 treated cells was higher than in AdNC treated cells (Fig. 5).

AdNR4A2 attenuates DMN reduced liver fibrosis. Further, we studied the effect of AdNR4A2 against DMN-induced liver fibrosis in rats. The rats were sacrificed and hepatic fibrosis was evaluated by hematoxylin and eosin, Sirius red and Masson's trichrome staining. The rats in AdNC (AdNC and DMN treated together) group and model (DMN treated only) group exhibited evident and uniform liver fibrosis after 4 weeks of repeated DMN injection. And most rats in the two groups showed stage 3 or 4 liver fibrosis. The severity of the liver fibrosis was markedly milder in the AdNR4A2 (AdNR4A2 and DMN treated together) group than that in AdNC group or model groups with most indicating stage 2 liver fibrosis (Fig. 6a and Supplementary Fig. S2).

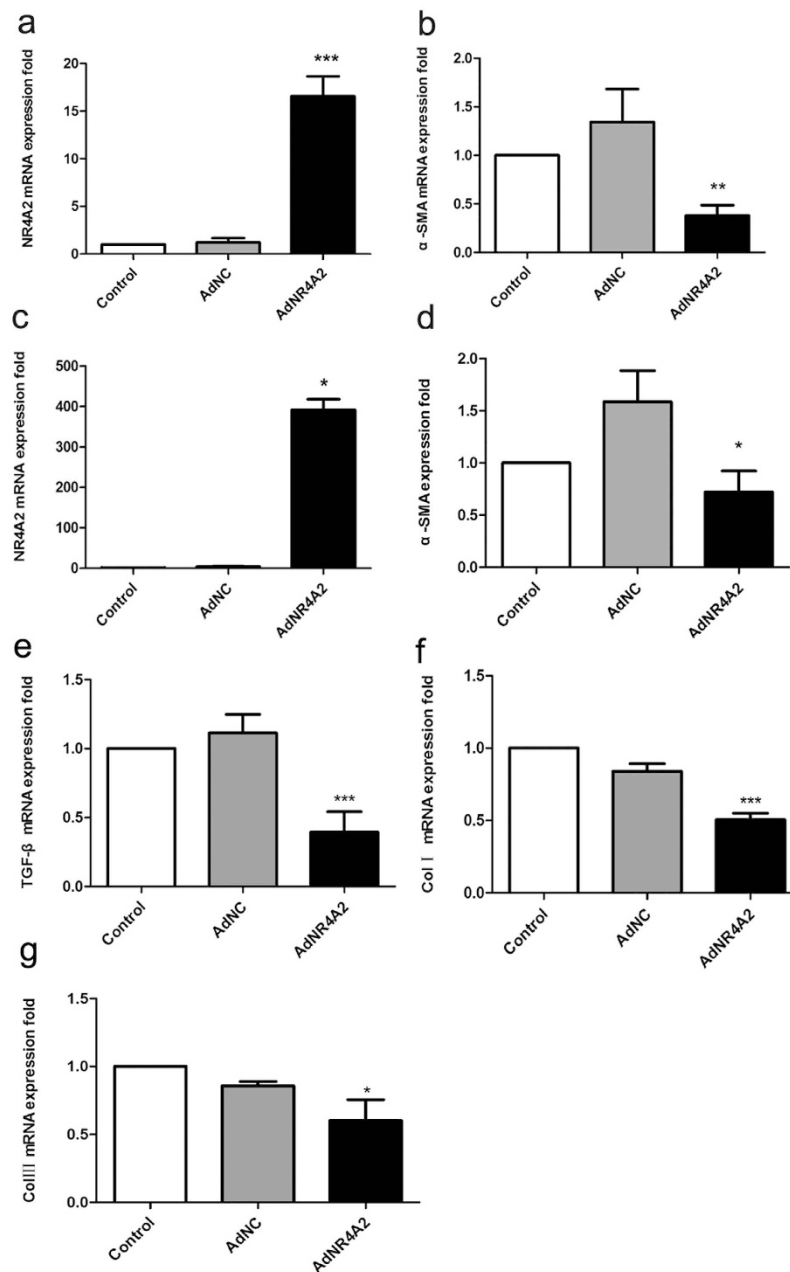


Figure 1. AdNR4A2 treatment causes increased NR4A2 expression and decreased α -SMA expression in hepatic stellate cells. HSC-T6 cells or rat primary hepatic stellate cells were treated with AdNR4A2 and AdNC respectively at an MOI of 40 for 72 hours. (a) The NR4A2 mRNA level in HSC-T6 cells. (b) The α -SMA mRNA level in HSC-T6 cells. (c) The NR4A2 mRNA level in rat primary hepatic stellate cells. (d) The α -SMA mRNA level in rat primary hepatic stellate cells. (e) The TGF- β mRNA level in HSC-T6 cells. (f) The Col I mRNA level in HSC-T6 cells. (g) The Col III mRNA level in HSC-T6 cells. The values are expressed as the mean \pm SD (n = 3). *p < 0.05, **p < 0.01 and ***p < 0.001 vs. AdNC group.

Fibrosis score for the Masson's trichrome staining suggested that fibrosis area increased significantly in AdNC group or model group after hepatic fibrosis was induced. At the same time the fibrosis area decreased evidently after AdNR4A2 treatment (Fig. 6b).

Hydroxyproline content, a commonly accepted indicator of fibrous tissue, was determined in the liver tissue. Accordance with the histological grading the liver hydroxyproline content of the AdNR4A2 group was significantly lower than that of AdNC group or model group, and there was no significant difference between AdNC group and model group (Fig. 6c).

RT-PCR analysis for mRNA of rat liver tissue indicated that α -SMA level increased obviously and NR4A2 level reduced sharply in model group or AdNC group than in normal group. The NR4A2 level elevated and α -SMA level reduced significantly in AdNR4A2 group compared with AdNC group or model group (Fig. 6d,e).

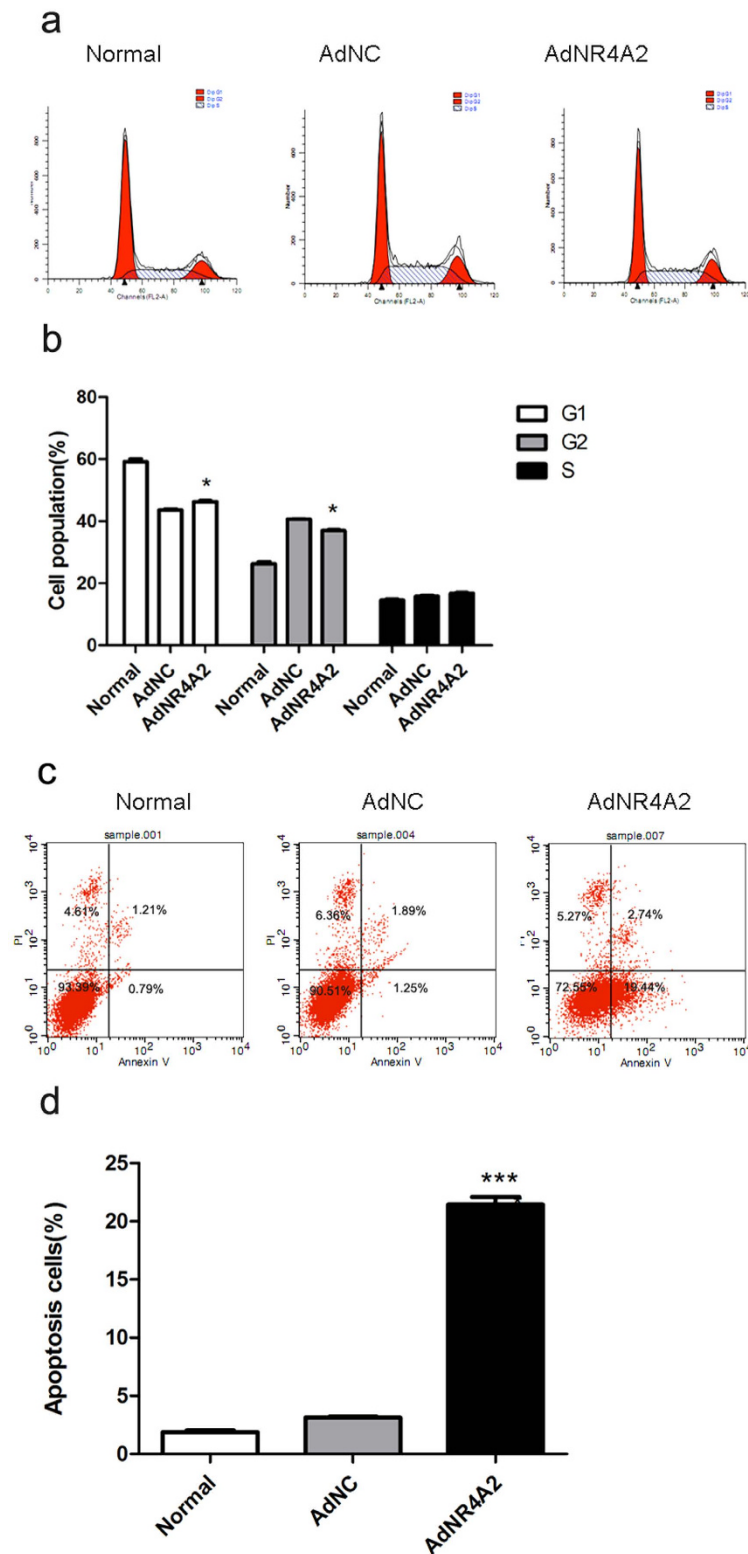


Figure 2. AdNR4A2 treatment causes cell cycle arrest and increased cell apoptosis rate. (a,b) HSC-T6 cells treated with AdNR4A2 and AdNC respectively at an MOI of 40 for 72 hours were stained with propidium iodide and analyzed by FACS to determine cell cycle. (a) Representative flow cytometry graph for control, AdNC and AdNR4A2 group. (b) Summary of cell cycle. (c,d) HSC-T6 cells treated with AdNR4A2 and AdNC respectively at an MOI of 40 for 72 hours were stained with propidium iodide and subjected to FACS analysis for determination of apoptotic cells. (c) Representative apoptosis graph for control, AdNC and AdNR4A2 group. (d) Summary of cell apoptosis. The values are expressed as the mean \pm SD ($n = 3$). * $p < 0.05$ and *** $p < 0.001$ vs. AdNC group.

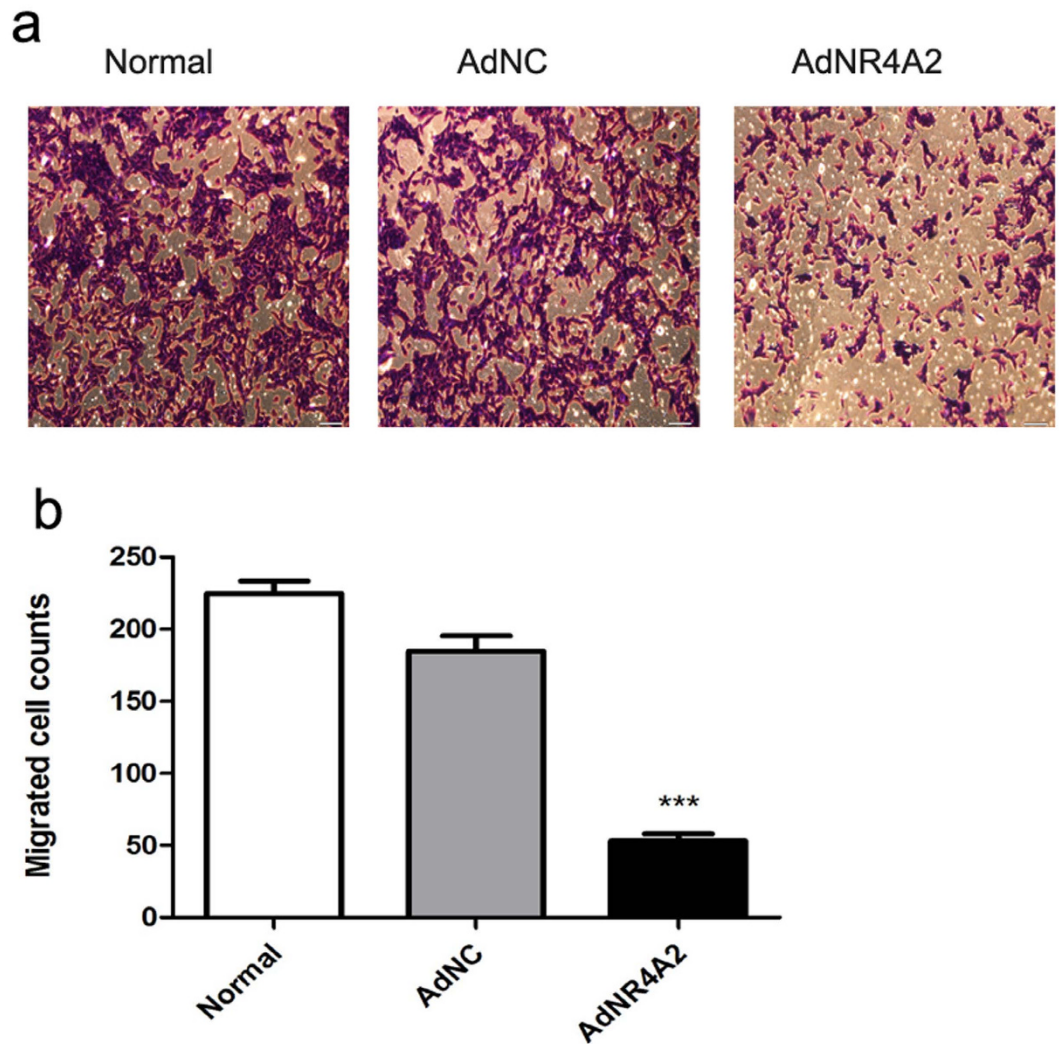


Figure 3. AdNR4A2 treatment inhibits the migration and invasion ability in hepatic stellate cells. HSC-T6 cells treated with AdNR4A2 and AdNC respectively at an MOI of 40 for 72 hours were subjected to transwell migration assay. (a) Representative Transwell graph for control, AdNC and AdNR4A2 group. (b) Analysis for the number of migrated cells. The values are expressed as the mean \pm SD (n = 3). ***p < 0.001 vs. AdNC group. Scale bar 200 μ m.

We detected the NR4A2 and α -SMA protein expression in liver tissue. Immunohistochemistry staining showed a sharp reduced staining of NR4A2 around portal tracts and in fibrotic septa after DMN injection. And the staining of NR4A2 increased significantly in AdNR4A2 group compared with AdNC group or model group (Fig. 7a). Immunofluorescence staining results revealed decreased staining of NR4A2 around portal tract and fibrotic septa after DMN injection, which was accompanied by increased α -SMA expression, implying that AdNR4A2 is involved in the inactivation of hepatic stellate cells. In consequence increased staining of NR4A2 accompanied by decreased expression of α -SMA was found in AdNR4A2 group than in AdNC group or model group (Fig. 7b and Supplementary Fig. S3). The staining of NR4A2 by double-label immunofluorescence in AdNR4A2 group was more intense than that in model group or AdNC group. There was no significant difference between model group and AdNC group (Fig. 7c). Meanwhile, the immunofluorescence of α -SMA in AdNR4A2 group exhibited lower density compared with model group or AdNC group (Fig. 7d).

To identify the effect of AdNR4A2 on apoptosis *in vivo*, we performed a staining for TUNEL in liver tissue. Of note, apoptotic cells were hardly observed in normal group. The number of apoptotic cells increased in model group or AdNC group after liver fibrosis was induced, but no variance occurred between them. And the number of apoptotic cells elevated significantly after AdNR4A2 treatment than in AdNC group or model group (Fig. 8a,b). These data implied that AdNR4A2 therapy may lead to the cell apoptosis *in vivo*.

Discussion

Liver fibrosis is the result of sustained hepatic inflammation and characterized with large amount of ECM in which HSCs play an important role. Quiet HSCs can be activated by a variety of insults. Activated HSCs secrete

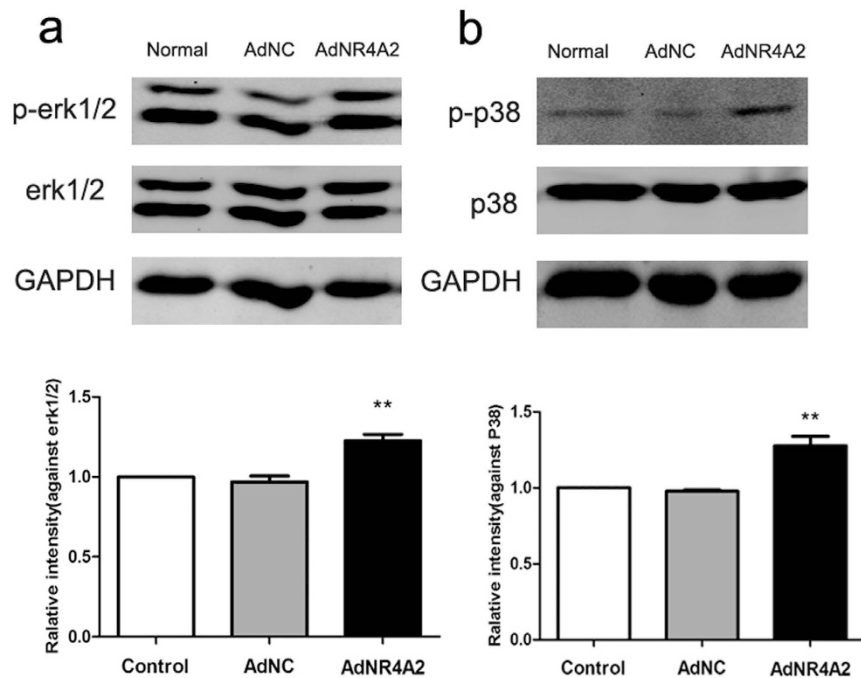


Figure 4. AdNR4A2 treatment increases the phosphorylation of ERK1/2 and P38 in hepatic stellate cells. Western blots were performed in HSC-T6 cells treated with AdNR4A2 and AdNC respectively at an MOI of 40 for 72 hours. (a) Western blot analysis on reducing blots and quantitative measurement of phosphorylation of ERK1/2. (b) Western blot analysis on reducing blots and quantitative measurement of phosphorylation of P38. The values are expressed as the mean \pm SD (n = 3). **p < 0.01 vs. AdNC group.

cytokines such as TGF- β , IL-6, IL-8, COX2 and TLR4. Among them TGF- β is a central regulator of mesenchymal repair responses and orchestrates the release of extracellular matrix during tissue repair¹⁷. Both reverting activated HSCs to quiet state or apoptosis and inhibiting profibrogenic gene expression of HSCs are effective for anti-fibrotic therapy. Recently it was demonstrated that liver fibrosis is reversible in either human being or animal model^{10–13}.

Accumulated evidence suggested nuclear receptors regulate key steps in activation of HSCs²¹. Peroxisome proliferator activated receptor- γ (PPAR- γ) inhibits profibrogenic genes expression in quiescent HSCs. Treatment with PPAR- γ agonists restrains HSCs from activation and suppresses collagen production^{22,23}. Our previous study indicated that NR4A2 level decreased significantly in fibrotic liver or activated HSCs and knockout of NR4A2 led to the increase of α -SMA and collagen I¹⁵. Our current study showed that NR4A2 gene over-expression resulted in the reduction of α -SMA in HSC-T6 cells. In addition, we obtained the same results in primary hepatic stellate cells. These cells could be spontaneously stimulated after isolation in which quiet HSCs transform into activated HSCs which resembles the activation process *in vivo*¹⁶.

TGF- β is a master regulator of mesenchymal responses in physiological and pathological conditions and induces the transcription of type I and III collagen in HSCs, promoting liver fibrosis¹⁷. Our previous study showed when HSCs were transiently stimulated by TGF- β the NR4A2 expression increased. Yet persistent stimulation led to reduced NR4A2 level¹⁵. We further demonstrated that NR4A2 over-expression resulted in decreased levels of TGF- β , Col I and Col III in HSCs. It implied that NR4A2 is a key checkpoint to control TGF- β signaling and chronically activated TGF- β signaling escapes the regulatory effects of NR4A2 by disrupting the NR4A2 feedback loop. Adenovirus mediated NR4A2 enhancement could re-activate an endogenous regulatory loop. When TGF- β expression was inhibited the levels of Col I and Col III reduced in the end. But the detailed mechanism needs to explore in future study.

NR4A2 is involved in regulating cell cycle and cell apoptosis²⁴. In our study, AdNR4A2 treatment led to cell cycle arrest such as increased percentage of cells in G1 phase and reduced percentage of cells in G2 phase as well as significant increase of cell apoptosis rate. It implied that NR4A2 enhancement could revert activated HSCs to quiet state via arresting cell cycle and promote cell apoptosis directly. This is consistent with documents that NR4As induces cell death apart from as transcription factor regulating target gene expression^{25–27}.

NR4A2 can relocate from nucleus to mitochondria and bind to Bcl-2 which triggers cytochrome C release and results in cell apoptosis²⁰. We applied adenovirus carrying NR4A2 to infect HSCs and found that the rate of NR4A2 nuclear translocation increased significantly. To a certain degree our study consistent with previous reports, but the mechanism and details require further exploration.

During liver fibrosis activated HSCs can migrate vigorously which is a distinctive property of activated HSCs²⁸. Our study showed that NR4A2 enhancement can weaken its migration and invasion ability. It illustrated that NR4A2 down-regulate the function of HSCs from another aspect.

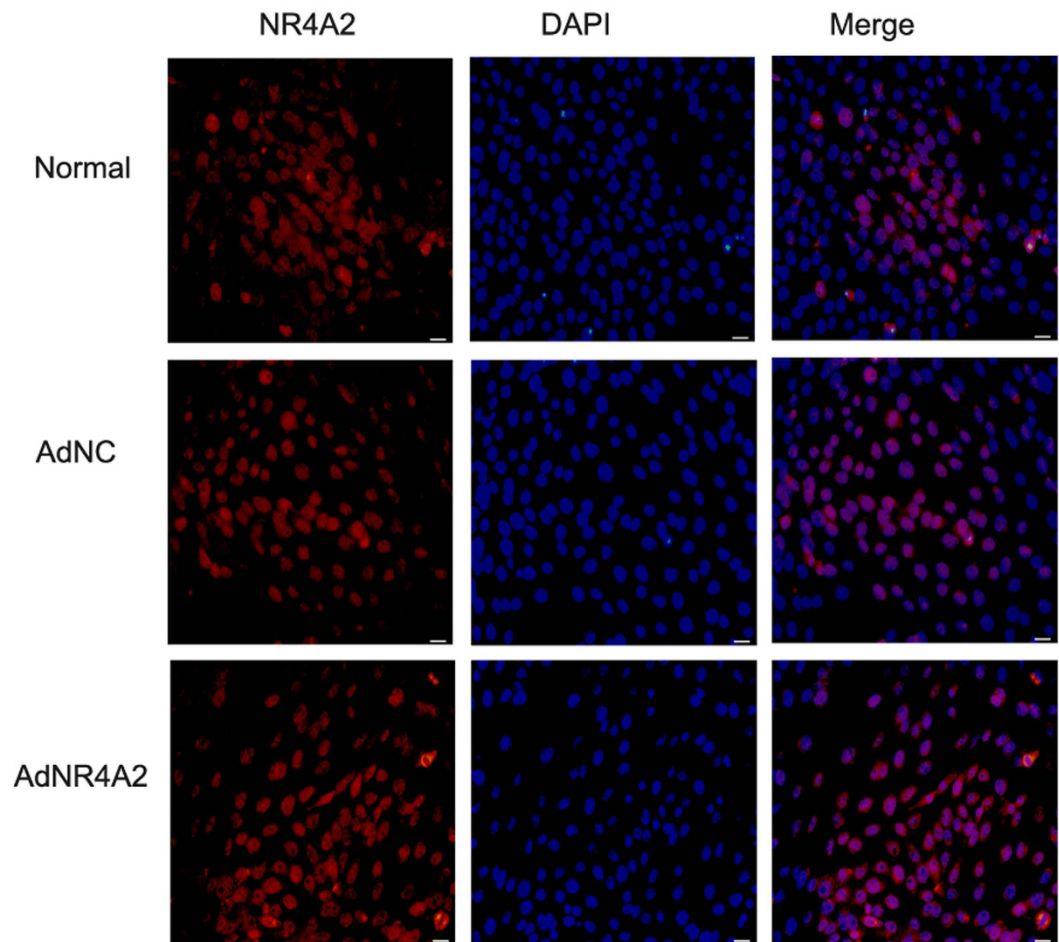


Figure 5. AdNR4A2 treatment leads the cytoplasmic translocation of NR4A2 in hepatic stellate cells. HSC-T6 cells treated with AdNR4A2 and AdNC respectively at an MOI of 40 for 72 hours were subjected to immunofluorescent costaining for NR4A2. Counterstaining was performed using DAPI for detection of nuclei. Cell fluorescence results showed cytoplasmic translocation of NR4A2 in HSC-T6 cells. Representative photomicrographs are shown at $\times 20$ magnification. scale bar $100\ \mu\text{m}$.

MAPK pathway is involved in the activation of HSCs and we previously found that knockdown of NR4A2 led to decrease of phosphorylation of MAPK. The Western blotting analysis showed reduced phosphorylation of ERK1/2, P38 and JNK when NR4A2 was knocked down in HSCs¹⁵. And on the contrary we observed NR4A2 gene over-expression in HSCs caused the increase of phosphorylation of ERK1/2 and P38. Glass *et al.* also reported that nuclear receptors were involved in regulation of signaling pathways and some nuclear receptors could inhibit inflammatory signaling pathways directly in macrophages and T cells²⁹. Our results are similar with Glass *et al.*'s. And it implied NRA42 may suppress the activation of HSCs via phosphorylation of MAPK pathway.

In addition we validated AdNR4A2 effect in liver fibrosis *in vivo*. Histological examination results showed AdNR4A2 therapy reverted fibrotic degree to stage 2 from stage 3 and decreased the collage content. Fibrosis score analysis indicated that the fibrotic area reduced sharply after AdNR4A2 treatment. We also observed that the NR4A2 protein and mRNA level reduced obviously and α -SMA levels elevated significantly when DMN was applied to induce liver fibrosis in rats. Meanwhile AdNR4A2 therapy gave rise to the increase of NR4A2 protein and mRNA level and the reduction of α -SMA protein and mRNA level. Taken together, AdNR4A2 treatment ameliorated liver fibrosis significantly *in vivo*. At the same time we noticed high expression of NR4A2 in hepatocytes in liver tissue. It is not contradictory as other cells express NR4A2 *in vivo*. Taura *et al.* demonstrated that hepatocytes are not involved in liver fibrogenesis³⁰. There were similar reports on NR4A member. Yin *et al.* discovered that the expression of NA4A1, NR4A2 and NR4A3 in leiomyoma was remarkably lower than that in myometrium and the reductions in NA4A2 and NR4A3 were significantly higher than NR4A1³¹. Our investigation is consistent with Yin *et al.* that NR4A2 level in fibrotic liver is lower compared with normal liver tissue. Leuprolide acetate is usually applied for the treatment of uterine fibroid. Yin *et al.* further found that Leuprolide acetate could suppress uterine fibrosis lesion via increasing NR4A2 level. In our study, we raised NR4A2 level through AdNR4A2 treatment *in vivo* and NR4A2 gene over-expression suppressed liver fibrosis in the end. It is evident that Yin *et al.*'s report strongly supports our view.

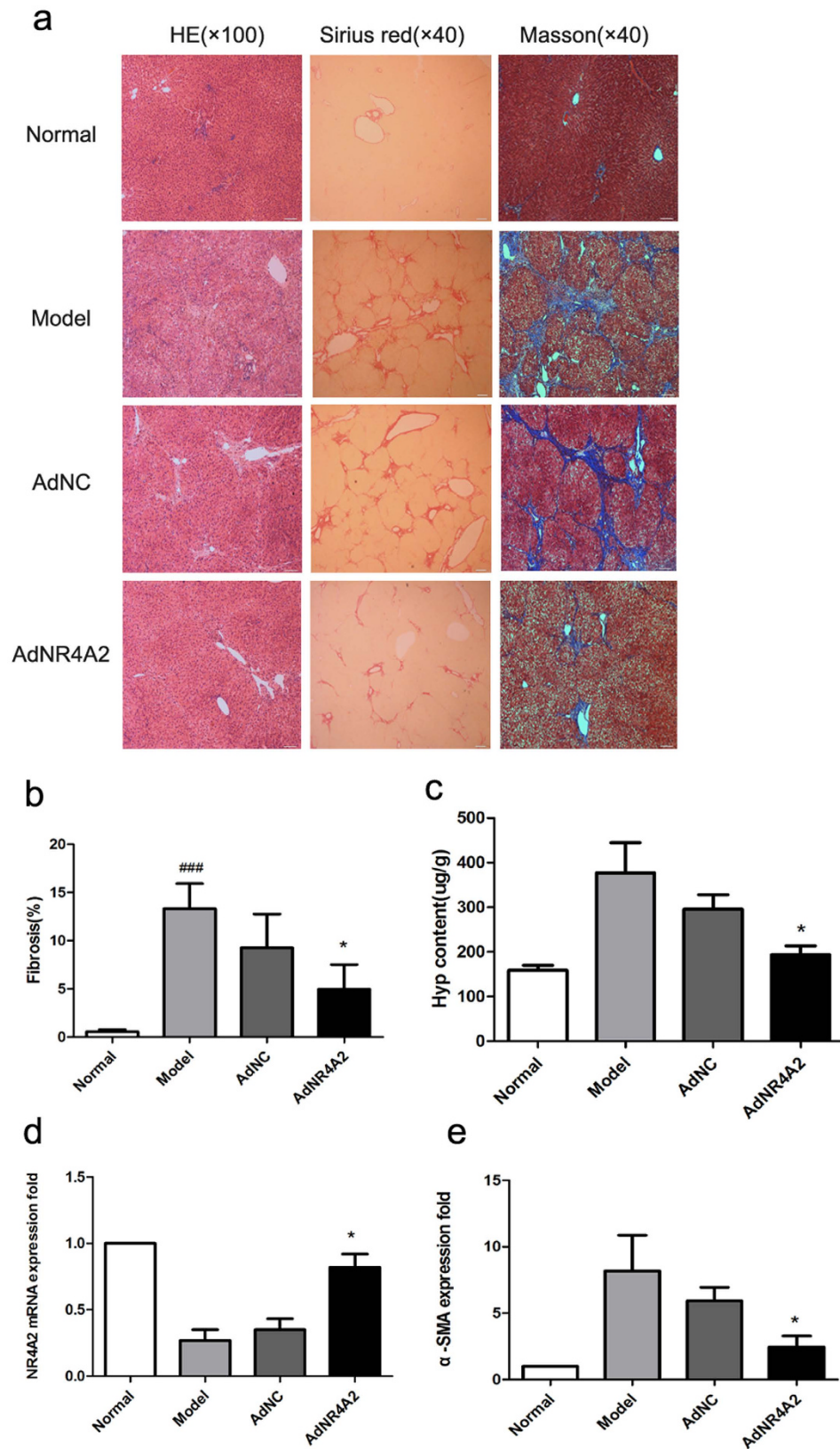


Figure 6. AdNR4A2 treatment alleviates dimethyl nitrosamine-induced liver fibrosis. Rats harboring dimethyl nitrosamine-induced hepatic fibrosis were treated by infusion of AdNR4A2, AdNC and medium respectively and sacrificed. The normal healthy rats were also sacrificed meantime. Paraffin-embedded liver sections were visualized by H/E staining, Sirius Red and Masson's trichrome staining and representative fields of view were photographed at $\times 4$ or $\times 10$ magnification. Stage 3 fibrosis is exemplarily shown in the medium-treated or AdNC-treated panel, as evidenced by fibrous bridges connecting portal tracts and central veins with

formation of multiple nodules whereas there was no fibrous tissue in normal healthy rat livers. The AdNR4A2-treated bottom panel is representative of stage 2 fibrosis, in which connective tissue links neighboring portal tracts while the overall architecture is preserved (a). (b) The Masson's trichrome staining results in normal rats, AdNR4A2 group, AdNC group and model group were subjected to fibrosis score analysis by computerized image morphometric analysis. (c) Collagen content (per g of liver) in normal rats, AdNR4A2 group, AdNC group and model group were measured by hydroxyproline biochemical determination. (d,e) mRNAs extracted from liver in normal group, AdNR4A2 group, AdNC group and model group were reverse-transcribed and used as template for quantitative real-time PCR (qPCR) to determine the relative NR4A2 and α -SMA expression level. AdNR4A2, AdNC and medium-treated samples and normal healthy sample were presented in terms of their relative expression level with respect to the normal control. (d) NR4A2 level in liver tissue. (e) α -SMA level in liver tissue. The values are expressed as the mean \pm SD (n = 6). *p < 0.05 vs. AdNC group. ***p < 0.001 vs. model group

NR4A2 involved in regulating cell cycle and cell apoptosis²⁴. We investigate the NR4A2 effect on apoptosis *in vivo*. Our study indicated that AdNR4A2 treatment increased the apoptosis rate in fibrotic liver. It suggested AdNR4A2 may abate liver fibrosis through promoting cell apoptosis *in vivo*.

In conclusion, our results showed NR4A2 gene over-expression could arrest cell cycle, promote cell apoptosis, deactivate MAPK pathway, weaken migration and invasion ability and reduce collagen production *in vitro*. In animal models AdNR4A2 treatment suppressed liver fibrosis obviously *in vivo*. These results suggest AdNR4A2 exhibit excellent anti-fibrotic effect. NR4A2 may be an ideal gene target for anti-fibrotic therapy and developing some agents increasing NR4A2 expression is very valuable for future clinical application.

Methods

Animals and treatments. Male Sprague-Dawley rats (SLAC, Shanghai, China), weighing approximately 250–270 g were maintained in a 12-hour dark/12-hour light cycle. The animal protocol was approved by the Animal Care and Use Committee of Shanghai Jiao Tong University Affiliated Sixth People's Hospital (License No. SYXK2011-0128). And all methods were performed in accordance with the relevant guidelines and regulations. The liver fibrosis model was induced by injection of DMN as described previously³². Normal group served as control which received intraperitoneal saline injection. Other group rats were injected intraperitoneally with 1% DMN (10 μ g/kg; Sigma, St. Louis, USA) for 3 consecutive days per week up to 4 weeks and infused with phosphate-buffered saline (model group), 5×10^9 pfu AdNR4A2 (AdNR4A2 group) or AdNC (AdNR4A2 group) via the tail vein respectively after six repeated DMN injection. The animals were sacrificed 4 weeks after DMN administration.

Adenovirus and cell lines. The HSC-T6 cells were kindly provided by Dr. Friedman of Mount Sinai School of Medicine of New York University (MSSM). Adenovirus targeting NR4A2 and its negative control (GenePharma, Shanghai, China) infected primary hepatic stellate cells or HSC-T6 cells at a multiplicity of infection of 40 for 72 hour. Cells were cultured in DMEM medium supplemented with 10% heat-inactivated fetal calf serum (FBS) (Gibco NY, USA). All cells were maintained in a humidified incubator at 37 °C with 5% CO₂.

Real time-polymerase chain reaction. Total RNA was purified from HSC cells or liver using Trizol (Takara, Dalian, China) and reverse transcribed was performed using PrimeScript RT Master Mix (Takara). Real time polymerase chain reaction (RT-PCR) was conducted by using SYBR Green PCR Kit (Takara) and Applied Biosystems 7500 real-time PCR system (Applied Biosystems, Foster City, CA, USA). Primer sequences (Sangon Biotech, Shanghai, China) were as follows: NR4A2 (Fw: 5'-AGATTCCTGGCTTTGCTGAC-3'; Rev: 5'-CTGGGTTGGACCTGTATGCT-3'); α -SMA (Fw: 5'-CCAGGGAGTGATGGTTGGA-3'; Rev: 5'-CCGTTAGCAAGGTCGGATG-3'); TGF- β (Fw: 5'-TGGCGTTACCTTGTAACC-3'; Rev: 5'-GGTGTGAGCCCTTCCAG-3'); Col I (Fw: 5'-AGGCATAAAGGGTCATCGTG-3'; Rev: 5'-ACCGTTGAGTCCATCTTTGC-3'); Col III (Fw: 5'-AGGCCAATGGCAATGTAAAG-3'; Rev: 5'-TATTGGTGGGTGAAACAGCA-3'); β -actin (Fw: 5'-ACCCACACTGTGCCCATCTATG-3'; Rev: 5'-AGAGTACTTGGCCTCAGGAGGA-3'). The resulting sequences were normalized to the β -actin expression levels, and relative gene expression was measured by the $2^{-\Delta\Delta CT}$ method.

Immunohistochemistry and immunofluorescence. Hepatic tissues were embedded in paraffin and sectioned. The sections were incubated in 3% H₂O₂ in methanol and nonspecific binding was blocked with 10% normal goat serum. The sections were incubated with primary antibody overnight, washed and incubated with secondary antibody for 60 minutes. Antigen-antibody complexes were visualized using DAB kits (GeneTech, Shanghai, China). Immunofluorescence was performed as described previously³³. The following primary antibodies were used: α -smooth muscle actin (α -SMA) (Santa Cruz), NR4A2 (Santa Cruz), Alexa Fluor[®] 546 IgG (Life Technologies), Alexa Fluor[®] 488 IgG (H + L) (Life Technologies). Image scanning analysis system (Image-Pro Plus) was used to analyze the changes in integrated optical density (IOD) of NR4A2 and α -SMA in immunofluorescence images.

Primary HSC isolation. Sprague-Dawley rats (SLAC, Shanghai, China) for primary HSCs were prepared. After anesthesia, the rat abdominal wall was opened and the intestines were moved aside so as to expose the vena cava and portal vein. A fine cannula ligated and fixed to a proper location was inserted into the vein after placing a thread around it. Perfusion solutions were incubated at 37 °C before usage. An adjustable peristaltic pump

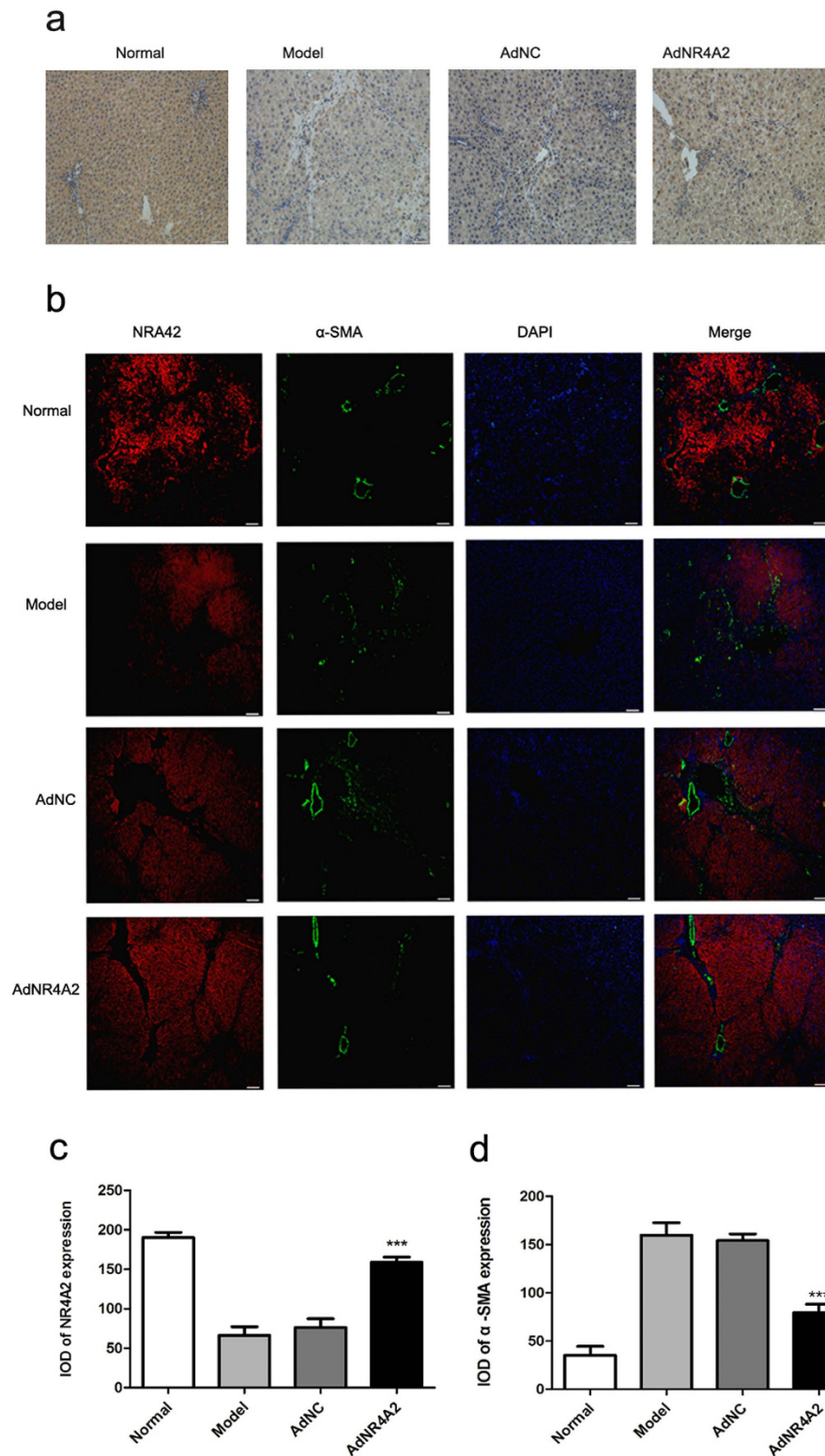


Figure 7. AdNR4A2 treatment increases NR4A2 level and decreases α -SMA level in dimethyl nitrosamine-induced fibrotic liver tissue. Rats harboring dimethyl nitrosamine-induced hepatic fibrosis were treated by infusion of AdNR4A2, AdNC and medium respectively and sacrificed. The normal healthy rats were also sacrificed meantime. Paraffin-embedded liver sections were made. **(a)** Immunohistochemical staining was performed with an antibody specific for NR4A2 and representative sections were imaged at $\times 20$ magnification. scale bar $100\mu\text{m}$. **(b)** Immunofluorescent costaining for NR4A2 and α -SMA. scale bar $200\mu\text{m}$. **(c,d)** The bar graphs showed the statistical results for NR4A2 and α -SMA expression in immunofluorescent images. The values are expressed as the mean \pm SD ($n = 6$). *** $p < 0.001$ vs. AdNC group.

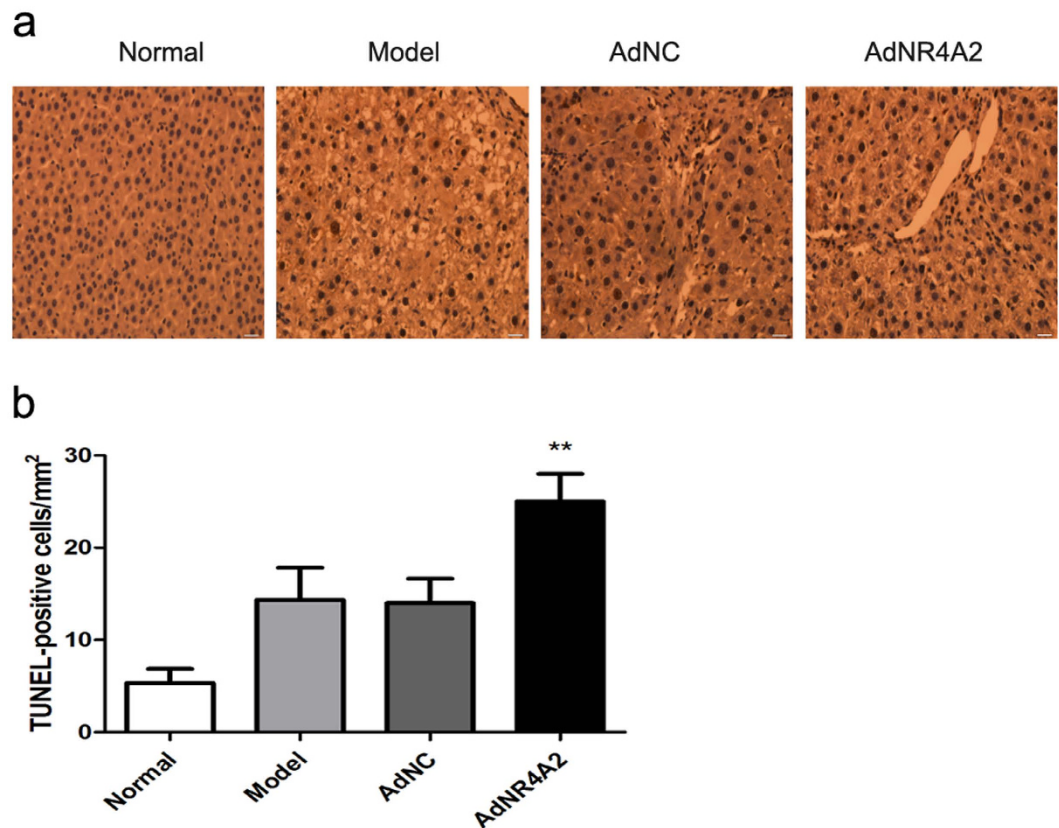


Figure 8. AdNR4A2 treatment promotes apoptosis *in vivo* in rats. Rats harboring dimethyl nitrosamine-induced hepatic fibrosis were treated by infusion of AdNR4A2, AdNC and medium respectively and sacrificed. The normal healthy rats were also sacrificed meantime. Paraffin-embedded liver sections were subjected to TUNEL assay. (a) Representative TUNEL graph for normal group, model group, AdNC group and AdNR4A2 group. (b) The number of apoptosis cells in liver tissue. The values are expressed as the mean \pm SD (n = 6). **p < 0.01 vs. AdNC group. scale bar 100 μ m.

was then used to control the *in situ* liver perfusion process. After the liver swelled, the cannula in the inferior vena cava was opened to allow draining. Subsequently, the liver was perfused in turn with D-Hank's solution, Collagenase IV solution, Pronase solution for 15 min at 37 °C. The cell fraction was collected, washed and put between a top layer of buffer and a bottom cushion of 18% Nycodenz. After centrifugation at 1400 g for 22 minutes, the HSCs fraction at the interface between the top and intermediate layer was obtained. Finally, the cells were cultured in DMEM medium supplemented with 10% FBS.

Western blot. Western blot analysis was performed as described previously³⁴. Western blots were performed using antibodies against GAPDH (Santa Cruz), IRDye680 anti-rabbit (Life Technologies), IRDye680 anti-mouse (Life Technologies), Erk1/2 (Cell Signaling, MA, USA), P-erk1/2 (Cell Signaling), P-P38 (Cell Signaling), P38 (Cell Signaling). Protein samples were transferred onto a polyvinylidene fluoride membrane and were scanned through Odyssey Infrared Imaging System.

Measurement of Hepatic Hydroxyproline Content. Total hepatic hydroxyproline levels Western blot analysis was determined according to standard protocols in the hydrolysates of liver samples as described³².

Cell cycle analysis. Cells were seeded into 6-well cell culture plates at a density of 5×10^5 cells. The cells were transfected with AdNR4A2 or AdNC respectively and 72 hour later the cells were harvested, stained and fixed with propidium iodide (PI) according to the manufacturer's protocol and subject to cell cycle analysis using flow cytometer (BD, NK, USA).

Cell apoptotic assay. Cells were seeded into 6-well cell culture plates at a density of 5×10^5 cells. The cells were transfected with AdNR4A2 or AdNC respectively and 72 hours later the cells were harvested. Apoptosis assay was measured using FITC Annexin V Apoptosis Detection Kit (Keygen, NJ, China) according to the manufacturer's protocol and subject to cell cycle analysis using flow cytometer.

Transwell migration assay. Transwell chambers (BD, Franklin Lakes, NJ, USA) were set up with 8-mm pore size filters to assess migration ability. HSC-T6 cells were harvested at the logarithmic phase and infected with

AdNR4A2 or AdNC respectively for 72 hour. Then cells were harvested and 0.2×10^5 cells were seeded onto the chamber's upper compartment with 200 μ l of serum-free medium and each group had 3 holes. At the same time, 500 μ l medium with 10% serum was added into the lower chamber. After 8 hour incubation at 37 °C and 5% CO₂ culture, the migrated cells would locate on the lower surface of the transwell filters. Then, these cells were fixed for 30 min in methanol and stained with 0.1% crystal violet for another 30 min. In each of 3 randomly selected sights under the microscope magnifying 200, the stained cells were observed and counted.

Histological Examination. All paraffin-embedded liver tissues were stained with hematoxylin and eosin, Sirius red staining and Masson's trichrome. Connective tissues stained blue with Masson's trichrome were measured on an image analyzer (Image J, National Institutes of Health). Three fields were selected randomly and six rats from each group were examined. The percentage was calculated as described previously³⁵.

Statistical analysis. The results were expressed as mean \pm SD and were analyzed by analysis of variance (ANOVA) or Student's t-test followed by paired comparison as appropriate. $P < 0.05$ was taken as the minimum level of significance.

References

- Schuppan, D. Structure of the extracellular matrix in normal and fibrotic liver: collagens and glycoproteins. *Semin Liver Dis* **10**, 1–10 (1990).
- Wake, K. Perisinusoidal stellate cells (fat-storing cells, interstitial cells, lipocytes), their related structure in and around the liver sinusoids and vitamin A-storing cells in extra hepatic organs. *Int Rev Cytol* **66**, 303–353 (1980).
- Choi, S. S. & Diehl, A. M. Epithelial-to-mesenchymal transitions in the liver. *Hepatology* **50**, 2007–2013 (2009).
- Okada, H., Strutz, F., Danoff, T. M., Kalluri, R. & Neilson, E. G. Possible mechanisms of renal fibrosis. *Contrib Nephrol* **118**, 147–154 (1996).
- Lee, J. M., Dedhar, S., Kalluri, R. & Thompson, E. W. The epithelial-mesenchymal transition: new insights in signaling, development and disease. *J Cell Biol* **172**, 973–981 (2006).
- Mederacke, I. *et al.* Fate tracing reveals hepatic stellate cells as dominant contributors to liver fibrosis independent of its aetiology. *Nat Commun* **4**, 2823 (2013).
- Geerts, A. History, heterogeneity, developmental biology and functions of quiescent hepatic stellate cells. *Semin Liver Dis* **21**, 311–335 (2001).
- Friedman, S. L. Hepatic stellate cells: protean, multifunctional, and enigmatic cells of the liver. *Physiol Rev* **88**, 125–172 (2008).
- Friedman, S. L., Roll, F. J., Boyles, J. & Bissell, D. M. Hepatic lipocytes: the principal collagen-producing cells of normal rat liver. *Proc Natl Acad Sci USA* **82**, 8681–8685 (1985).
- Ramachandran, P. & Iredale, J. P. Reversibility of liver fibrosis. *Ann Hepatol* **8**, 283–291 (2009).
- Henderson, N. C. & Iredale, J. P. Liver fibrosis: cellular mechanisms of progression and resolution. *Clin Sci* **112**, 265–280 (2007).
- Mallet, V. *et al.* Brief communication: The relationship of regression of cirrhosis to outcome in chronic hepatitis C. *Ann Intern Med* **149**, 399–403 (2008).
- Friedman, S. L. & Bansal, M. B. Reversal of hepatic fibrosis—factor fantasy? *Hepatology* **43**, S82–S88 (2006).
- Bansal, R. *et al.* Engineered targeted interferon-gamma blocks hepatic fibrogenesis in mice. *Hepatology* **54**, 586–596 (2011).
- Chen, P. *et al.* Orphan nuclear receptor NR4A2 inhibits hepatic stellate cell proliferation through MAPK pathway in liver fibrosis. *PeerJ* **3**, e1518 (2015).
- Davis, B. H. & Vucic, A. The effect of retinol on Ito cell proliferation *in vitro*. *Hepatology* **8**, 788–793 (1988).
- Hernandez-Gea, V. & Friedman, S. L. Pathogenesis of liver fibrosis. *Annu Rev Pathol* **6**, 425–456 (2011).
- Martinez-Hernandez, A. & Amenta, P. S. The extracellular matrix in hepatic regeneration. *FASEB J* **9**, 1401–1410 (1995).
- Saxena, N. K. *et al.* Concomitant activation of the JAK/STAT, PI3K/AKT, and ERK signaling is involved in leptin-mediated promotion of invasion and migration of hepatocellular carcinoma cells. *Cancer Res* **67**, 2497–2507 (2007).
- Deutsch, A. J., Angerer, H., Fuchs, T. E. & Neumeister, P. The Nuclear Orphan Receptors NR4A as Therapeutic Target in Cancer Therapy. *Anti-Cancer Agents in Medicinal Chemistry* **12**, 1001–1014 (2012).
- Hellemans, K. *et al.* Differential modulation of rat hepatic stellate phenotype by natural and synthetic retinoids. *Hepatology* **39**, 97–108 (2004).
- Chen, H., He, Y. W., Liu, W. Q. & Zhang, J. H. Rosiglitazone prevents murine hepatic fibrosis induced by *Schistosoma japonicum*. *World J Gastroenterol* **14**, 2905–2911 (2008).
- Yang, L., Stimpson, S. A., Chen, L., Wallace Harrington, W. & Rockey, D. C. Effectiveness of the PPAR- γ agonist, GW570, in liver fibrosis. *Inflamm Res* **59**, 1061–1071 (2010).
- Zhao, D., Desai, S. & Zeng, H. VEGF stimulates PKD-mediated CREB-dependent Orphan nuclear receptor Nurr1 expression: role in VEGF-induced angiogenesis. *International Journal of Cancer* **128**, 2602–2612 (2011).
- Li, H. *et al.* Cytochrome c release and apoptosis induced by mitochondrial targeting of nuclear orphan receptor TR3. *Science* **289**, 1159–1164 (2000).
- Moll, U. M., Marchenko, N. & Zhang, X. K. p53 and Nur77/TR3 -transcription factors that directly target mitochondria for cell death induction. *Oncogene* **25**, 4725–4743 (2006).
- Thompson, J. & Winoto, A. During negative selection, Nur77 family proteins translocate to mitochondria where they associate with Bcl-2 and expose its proapoptotic BH3 domain. *J Exp Med* **205**, 1029–1036 (2008).
- Friedman, S. L. Evolving challenges in hepatic fibrosis. *Nat Rev Gastroenterol Hepatol* **7**, 425–436 (2010).
- Glass, C. K. & Saijo, K. Nuclear receptor transrepression pathways that regulate inflammation in macrophages and T cells. *Nat Rev Immunol* **10**, 365–376 (2010).
- Taura, K. *et al.* Hepatocytes do not undergo epithelial-mesenchymal transition in liver fibrosis in mice. *Hepatology* **51**, 1027–1036 (2010).
- Yin, H. *et al.* Expression profiling of nuclear receptors identifies key roles of NR4A subfamily in uterine fibroids. *Molecular Endocrinology* **27**, 726–740 (2013).
- Lin, Y. *et al.* Treatment of experimental hepatic fibrosis by combinational delivery of urokinase-type plasminogen activator and hepatocyte growth factor genes. *Liver Int* **25**, 796–807 (2005).
- García-Pérez, D. *et al.* Morphine regulates Argonaute2 and TH expression and activity but not miR-133b in midbrain dopaminergic neurons. *Addict Biol* **20**, 104–119 (2015).
- Ogawa, T. *et al.* MicroRNA-221/222 upregulation indicates the activation of stellate cells and the progression of liver fibrosis. *Gut* **61**, 1600–1609 (2012).
- Guimond, A. *et al.* Quantitative ultrasonic tissue characterization as a new tool for continuous monitoring of chronic liver remodeling in mice. *Liver Int* **27**, 854–864 (2007).

Acknowledgements

The study was supported by grants from National Natural Science Foundation (81072687) and Shanghai Committee of Science and Technology (14ZR1432200).

Author Contributions

P.C. conceived and performed the experiments, wrote the main manuscript. J.L., Y.H., J.L., L.W. and Q.Y. performed experiments. J.H. and R.G. prepared Figures and analyzed the data. C.G. conceived the experiments and wrote the main manuscript. All authors reviewed the manuscript.

Additional Information

Supplementary information accompanies this paper at <http://www.nature.com/srep>

Competing financial interests: The authors declare no competing financial interests.

How to cite this article: Chen, P. *et al.* Adenovirus-mediated expression of orphan nuclear receptor NR4A2 targeting hepatic stellate cell attenuates liver fibrosis in rats. *Sci. Rep.* **6**, 33593; doi: 10.1038/srep33593 (2016).



This work is licensed under a Creative Commons Attribution 4.0 International License. The images or other third party material in this article are included in the article's Creative Commons license, unless indicated otherwise in the credit line; if the material is not included under the Creative Commons license, users will need to obtain permission from the license holder to reproduce the material. To view a copy of this license, visit <http://creativecommons.org/licenses/by/4.0/>

© The Author(s) 2016